

Deuterium NMR and Differential Scanning Calorimetric Studies of the Calcium Salts of Rhodium and Iridium Pentadeuterides, Ca_2RhD_5 and Ca_2IrD_5

Denis F. R. Gilson,^{*,†} Frederick G. Morin,[†] and Ralph O. Moyer, Jr.[‡]

Department of Chemistry, McGill University, 801 Sherbrooke Street, W., Montreal, QC H3A 2K6 Canada, and
Department of Chemistry, Trinity College, Hartford, Connecticut 06106-3100

Received: April 21, 2006; In Final Form: June 29, 2006

The deuterium NMR spectra of the ternary metal deuterides (TMDs) Ca_2RhD_5 and Ca_2IrD_5 show that the disorder is dynamic at room temperature, with barriers to the motion of 31.8 and 39.0 kJ mol⁻¹, respectively. At low temperatures, splittings equivalent to quadrupole coupling constants of 50.9 and 24.5 kHz were obtained for Ca_2RhD_5 and 68.3 and 41.7 kHz for Ca_2IrD_5 and are assigned to the planar and apical deuterium positions, respectively. Differential scanning calorimetric study of the transition in Ca_2IrH_5 located a reversible phase transition at 284 K with an enthalpy change of 650 J mol⁻¹ and entropy change of 2.3 J K⁻¹ mol⁻¹.

Introduction

The properties of metal hydrides are of considerable practical interest as materials useful for hydrogen storage devices,¹ as catalysts, and also for their unique chemical bonding patterns.² The ternary metal hydride (TMH) salts of transition metals with alkali metals or alkaline earths exhibit complicated stoichiometries and geometries. For example, the rhodium and iridium TMHs, the transition metals of interest in the present study, have been reported as Li_3RhH_4 , Li_3RhH_6 , Na_3RhH_6 , Ca_2RhH_5 , $\text{Ca}_8\text{Rh}_5\text{H}_{23}$ and $\text{Ca}_8\text{Rh}_6\text{H}_{24}$, Sr_2RhH_5 , $\text{Sr}_8\text{Rh}_5\text{H}_{23}$,^{3–10} and Li_3IrH_6 , Na_3IrH_6 , Ca_2IrH_5 , Sr_2IrH_5 , and $\text{Mg}_4\text{IrH}_{11}$,^{5,7,11–14} Mg_2IrH_5 , $\text{Mg}_3\text{IrH}_{11}$, and $\text{Mg}_6\text{Ir}_2\text{H}_{11}$.^{5,7,11–14} These compounds are synthesized by two different solid-state methods: either by forming the binary metal alloy at high temperature and then subjecting it to a high pressure of hydrogen, again at high temperature, or by heating the alkali or alkaline earth hydride with the transition metal in an atmosphere of hydrogen. The initial relative concentrations of the metals and reaction conditions are important in determining the final products.

The structural properties of the TMH salts have been investigated by X-ray powder diffraction methods or by neutron diffraction in the case of deuteride compounds.^{8,9,11,12} The structures of the calcium salts of rhodium and iridium pentadeuteride, Ca_2RhD_5 and Ca_2IrD_5 , have been previously reported.¹² At room temperature, the anion structures, $[\text{MD}_5]^{4-}$, are disordered octahedra with 5/6 occupancy of the six coordination sites. As the temperature is lowered, Ca_2IrD_5 undergoes a phase transition, between 295 and 275 K, going from a face-centered-cubic (space group $Fm\bar{3}m$, K_2PtCl_6 -type) to a tetragonal structure, space group $I4/mmm$, in which four deuterium atoms now fully occupy the equatorial sites and the two apical sites are half-occupied. The strontium analogue, Sr_2IrD_5 , also undergoes the same cubic-to-tetragonal transition between 200 and 140 K, but is incomplete even down to 4.2 K.¹¹ Structurally similar mixed crystal TMHs of europium with calcium and strontium show similar transitions between 200 and

240 K.¹⁵ Ca_2RhH_5 , however, remains in the disordered cubic phase from room temperature to 20 K. Except for these structural studies, no other physical measurements have been reported for the rhodium and iridium TMHs. It is not known whether the disorder in the cubic phase is static or dynamic. To address this problem, we have investigated the deuterium NMR spectra of these compounds as a function of temperature and examined the thermal behavior by differential scanning calorimetry (DSC).

Experimental Section

All TMDs were prepared by previously reported methods,^{7,12} namely, purification of the calcium metal by high-temperature vacuum distillation and then the subsequent formation of the binary deuteride by direct reaction of the purified metal with the gas at high temperatures. Powders of the deuterides were then mixed with the transition metal powders (–325 mesh) in the mole ratios of 2:1 and heated at 700 °C in approximately 1 atm pressure of deuterium gas. The purities were confirmed by powder X-ray diffraction methods.

DSC measurements were made for both Ca_2IrH_5 and Ca_2IrD_5 using a TA Instruments Q1000 DSC equipped with a refrigerated cooling system (RCS) and calibrated using an indium reference. Samples were contained in sealed aluminum pans and scanned at a rate of 10 °C/min.

Deuterium NMR spectra were obtained with a Chemagnetics CMX-300 spectrometer at an operating frequency of 45.9 MHz, using the quadrupole-echo method.¹⁶ Pulse widths of 4 μs at high temperatures and 7 μs at low temperatures were used with a delay time of 25 μs , and recycle delays varied from 20 to 300 s, depending on the temperature. The low-temperature spectra of Ca_2RhD_5 were obtained with 8 or 16 scans, and those of Ca_2IrD_5 were obtained with 32 scans. Spin–lattice relaxation times were measured by inversion recovery or by saturation recovery methods. A Gaussian broadening of 500 Hz was applied before Fourier transform.

Results and Discussion

DSC Measurements. The onset temperatures of the phase transition in Ca_2IrH_5 were 286 K on cooling and 282 K on heating. Cycling through the transition showed it to be revers-

* Corresponding author. Fax: 1-514-398-3797. E-mail: denis.gilson@mcgill.ca.

[†] McGill University.

[‡] Trinity College.

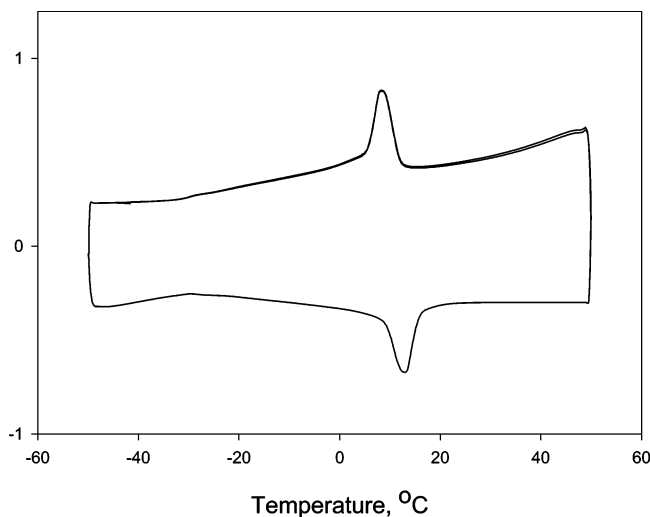


Figure 1. DSC scans for Ca_2IrH_5 . The initial scan from 50 to -50°C was followed by an increase to 50°C and decrease again to -50°C .

ible, Figure 1. The results for Ca_2IrD_5 were identical. The transition temperature is consistent with the neutron diffraction studies of changes in the unit cell dimensions occurring between 275 and 295 K.¹² Enthalpy changes were 603 and 695 J mol^{-1} , and entropy changes were 2.1 and 2.5 $\text{J K}^{-1} \text{mol}^{-1}$ on cooling and heating, respectively. The entropy change expected for a transition from 5 atoms disordered over 6 sites to one atom disordered between two sites, $\Delta S = R \ln[(5/6)/(1/2)]$, is 4.2 $\text{J K}^{-1} \text{mol}^{-1}$.

Deuterium NMR Measurements. For a rigid case, the deuterium NMR spectrum consists of a “Pake doublet” in which the splitting is given by $(3/4)(C_Q)$ where $C_Q = e^2Qq/h$ is the nuclear quadrupole coupling constant. If the frequency of the motion exceeds the coupling constant, then the structure of the Pake doublet disappears. At room temperature, the ^2H NMR spectra of Ca_2RhD_5 and Ca_2IrD_5 both showed sharp single peaks, Figures 2 and 3. In the case of Ca_2RhD_5 , the single peak was accompanied by a weak Pake doublet. The sharp singlets indicate that the disorder is dynamic, presumably by a vacancy-hopping mechanism, and at temperatures above ambient the spin lattice relaxation times were short enough to measure easily.

In the case of quadrupolar relaxation, the spin–lattice relaxation time, T_1 , is given by¹⁷

$$1/T_1 = (3\pi^2/10)(C_Q)^2(1 + \eta^2/3)\tau_c \{ 1/(1 + \omega^2\tau_c^2) + 4/(1 + 4\omega^2\tau_c^2) \} \quad (1)$$

where η is the asymmetry parameter, ω is the resonance frequency, and the correlation time for the motion, τ_c , is given by $\tau_0 \exp(E/RT)$. Two regimes exist, depending on whether $\omega^2\tau_c^2$ is much greater or much less than unity, that is, a slow or fast motion is involved, and a plot of $\ln(T_1)$ versus reciprocal temperature allows the determination of the barrier to motion. The results for Ca_2RhD_5 and Ca_2IrD_5 for the temperature ranges 293–413 K and 294–398 K, respectively, are shown in Figure 4. Barriers of 39.0 and 32.0 kJ mol^{-1} , respectively, were obtained, and the motion is clearly in the slow collision region. As the temperature was decreased below room temperature, the

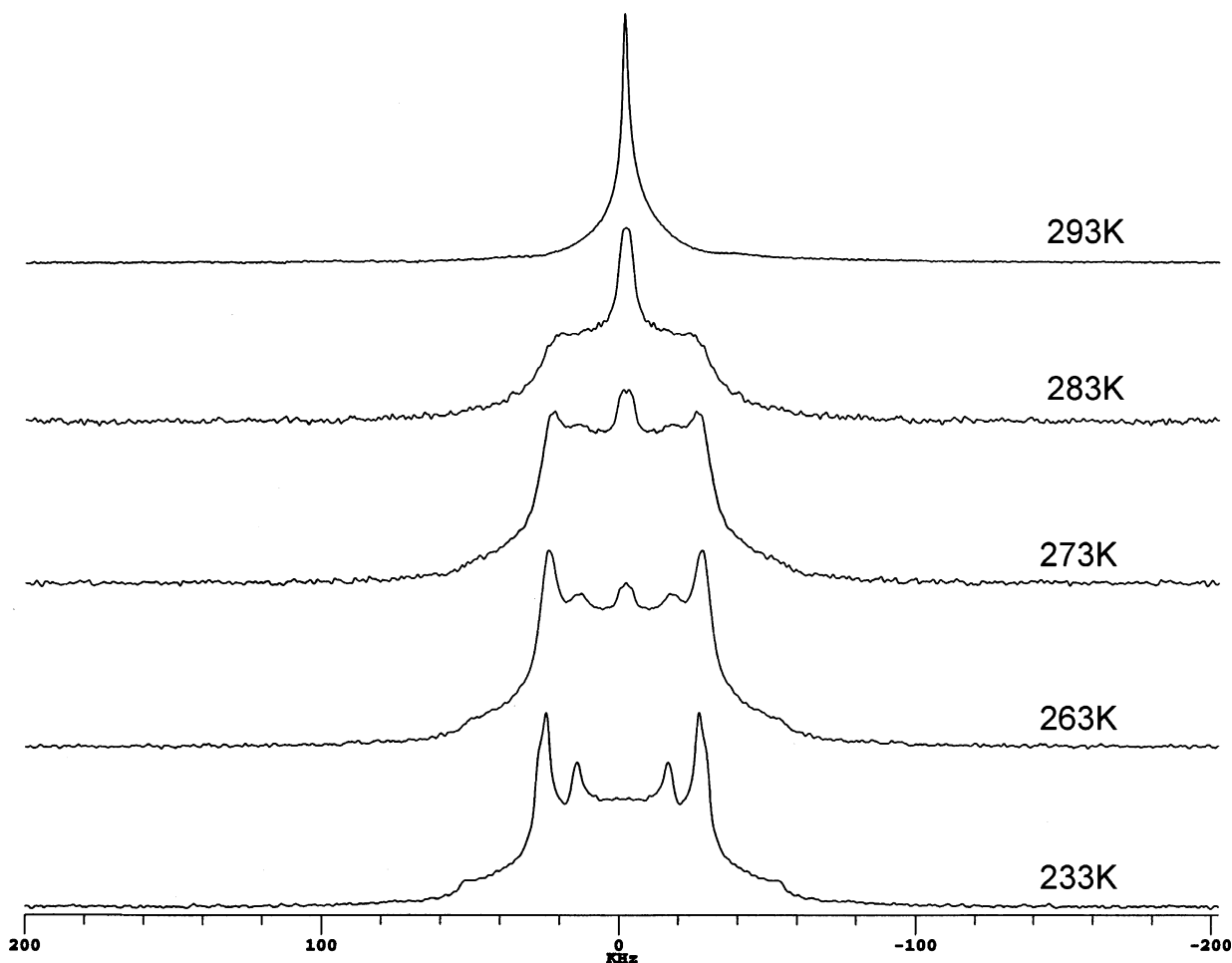


Figure 2. Temperature dependence of the ^2H NMR spectra of Ca_2IrD_5 .

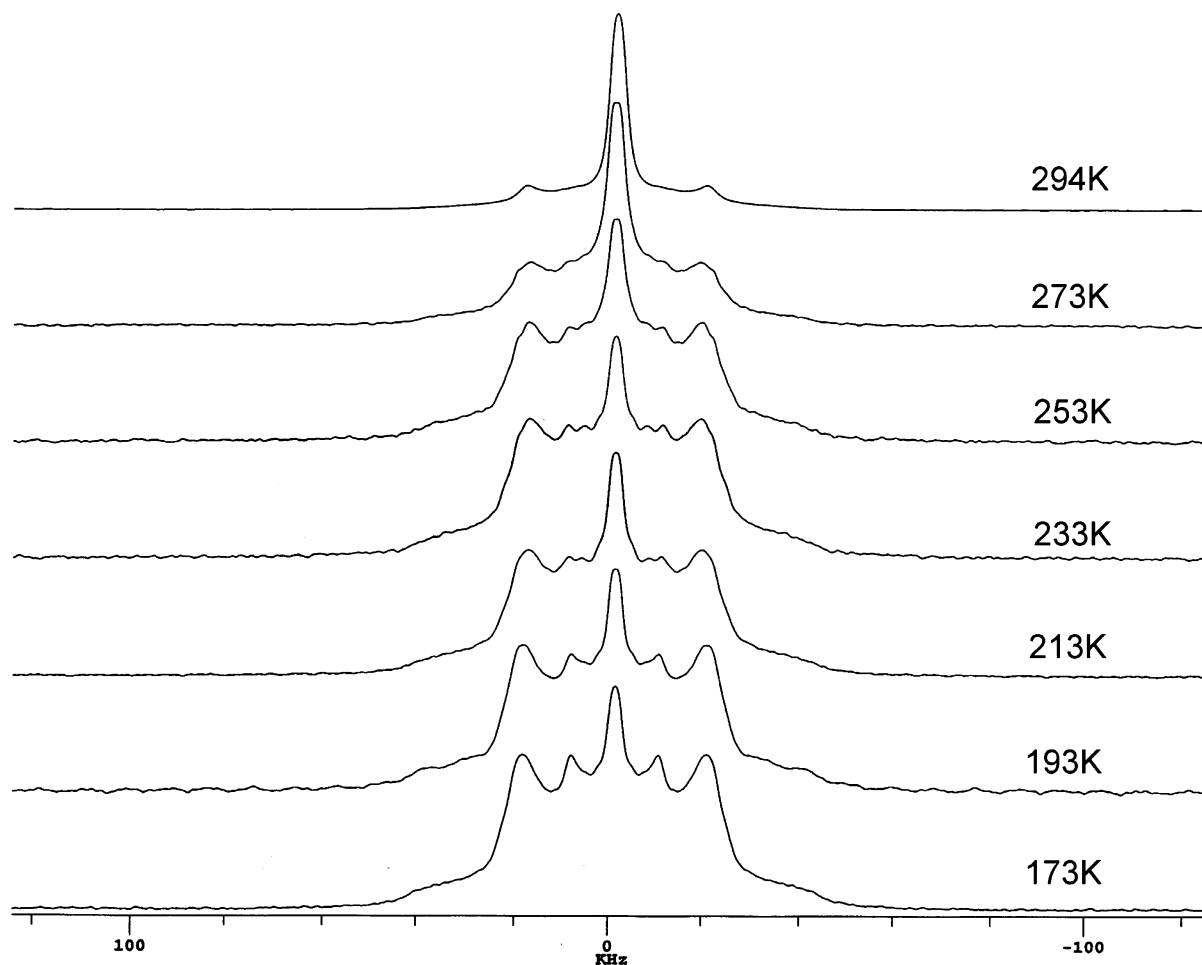


Figure 3. Temperature dependence of the ^2H NMR spectra of Ca_2RhD_5 .

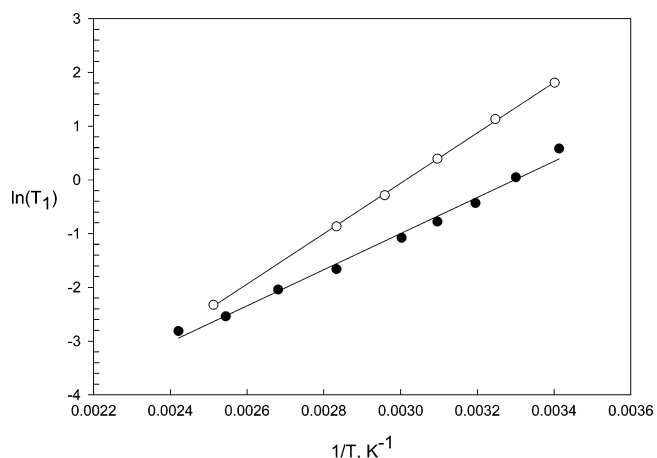


Figure 4. Plots of $\ln(1/T_1)$ versus reciprocal temperature for Ca_2IrD_5 (open circles) and Ca_2RhD_5 (filled circles).

spectrum of Ca_2IrD_5 broadened and, below the phase transition, consisted of two overlapping Pake doublets, Figure 2, with splittings of 51.2 and 31.3 kHz. The outer, more intense doublet is assigned to the four deuterium atoms in the equatorial sites with a quadrupole coupling constant of 68.3 kHz, and the inner doublet is assigned to the apical site with a coupling constant of 41.7 kHz. For Ca_2RhD_5 , however, a more complicated behavior was observed. With decreasing temperature, the intensity of the narrow line decreased and two then three Pake doublets increased in intensity. But on further decrease in

temperature to below 190 K only two doublets, plus the singlet, remained, Figure 3. The quadrupole coupling constants of these two doublets were 50.9 and 24.5 kHz. The very large differences in T_1 for each of the peaks made it impossible to determine the relative intensities of each species.

This behavior is consistent with the previous studies¹² demonstrating the absence of a phase transition in the rhodium compound and, at low temperatures, motion in the rhodium TMD slows until a statistically disordered state is attained. In contrast, the transformation of the cubic phase of Ca_2IrD_5 to the tetragonal phase must be cooperative in nature.

The three different forms described for the calcium rhodium hydride system, Ca_2RhH_5 , $\text{Ca}_8\text{Rh}_5\text{H}_{23}$, and $\text{Ca}_8\text{Rh}_6\text{H}_{24}$,^{8,9,12} have 2, 4, and 2 different Rh–H(D) bond lengths, respectively, and, therefore, should have 2, 4, and 2 different nuclear quadrupole coupling constants. In the present study, only two quadrupole splittings were observed in agreement with the Ca_2RhH_5 or $\text{Ca}_8\text{Rh}_6\text{H}_{24}$ formulation, but the bond length of the apical Rh–H bond in $\text{Ca}_8\text{Rh}_6\text{H}_{24}$ is shorter than those in the equatorial plane, which should result in the larger C_Q value, in disagreement with the observed spectrum.

Values of the deuterium quadrupole coupling constants for transition metal systems are more commonly derived from the T_1 minima obtained via solution-phase measurements.¹⁸ For terminal transition metal deuterides, as opposed to bridging hydrides or dihydrogen ligands, the values typically lie in the range 30 to 100 kHz, with occasional exceptions at much higher frequency.¹⁸ The values obtained in the present study are at the lower end of the range. However, there will be

differences between the quadrupole coupling constants measured in the solid phase and those obtained from solution measurements.

Berke and co-workers^{18–20} have proposed that the deuterium quadrupole coupling constants can be used to derive the ionic character of the deuterium–metal bond. The treatment is based upon the Townes and Dailey theory,²¹ eq 2,

$$q_{\text{mol}} = (1 - S)(1 - I)q_{\text{at}} \quad (2)$$

where q_{mol} and q_{at} are the electric field gradients in the molecule and the atom, respectively, S is the s-character, and I is the ionic character of the bonding orbital. If the q_{at} term is replaced by the field gradient for the D_2 molecule, then eq 2 can be rewritten as eq 3:

$$(C_Q)_{\text{M-D}} = (1 - I)(C_Q)_{\text{D-D}} \quad (3)$$

Implicit in eq 3 is the assumption that the s-character in the metal–deuterium bond is less than 100% and is the same as that in the deuterium–deuterium bond. Using the value of 227 kHz for the quadrupole coupling constant in deuterium, then the ionic characters are 78 and 89% for the equatorial and apical deuterium in Ca_2IrD_5 , and 70 and 82% in Ca_2RhD_5 . Values for a variety of transition metal hydride complexes range from 67 to 85%,¹⁸ and the ionic character of the apical bond is clearly at the higher limit. However, the differences between the quadrupole coupling constant values derived from solution and from solid-state measurements must be considered.²²

Firman and Landis,²³ using Sr_2RhH_5 and Sr_2IrH_5 as examples, have proposed that the structure should be formulated as a resonance structure between the 18-electron mono-vacancy ion, where two electrons are transferred from each strontium ion to the transition metal, and a 16-electron square planar ion where only one electron is transferred. In the first case, it is predicted that a hydride ion is ejected to an interstitial site leaving a square planar $[\text{Rh-H}_4]^{3-}$ ion. The Sr^+ form would predict that the apical bond is shorter than the equatorial bonds. The low-temperature neutron diffraction structures of Sr_2IrD_5 ¹¹ and Ca_2 -

IrD_5 ¹² both show the apical bond to be longer. The higher ionic character of the apical bond is consistent with this picture.

Acknowledgment. R.O.M. acknowledges financial support from the Trinity College Scovill Chair Research Fund and the hospitality of McGill University during a sabbatical leave. We thank Petr Fiurasek (Centre for Self-Assembled Chemical Structures) for assistance with the DSC measurements.

References and Notes

- (1) Schluplach, L.; Züttel, A. *Nature* **2001**, *414*, 353.
- (2) McGrady, G. C.; Guiler, G. *Chem. Soc. Rev.* **2003**, *32*, 383.
- (3) Bronger, W.; Mueller, P.; Kowalczyk, J.; Auffermann, G. *J. Alloys Compds.* **1991**, *176*, 263.
- (4) Bronger, W.; Gehlen, M.; Auffermann, G. *Z. Anorg. Allg. Chem.* **1994**, *620*, 1983.
- (5) Bronger, W.; Gehlen, M.; Auffermann, G. *J. Alloys Compds.* **1991**, *176*, 255.
- (6) Heckers, U.; Niewa, R.; Jacobs, H. *Z. Anorg. Allg. Chem.* **2001**, *627*, 1401.
- (7) Moyer, R. O., Jr.; Stanitski, C.; Tanaka, J.; Kay, M. I.; Kleinberg, R. *J. Solid State Chem.* **1971**, *3*, 541.
- (8) Bronger, W.; Jansen, K.; Breil, L. *Z. Anorg. Allg. Chem.* **1998**, *624*, 1477.
- (9) Bronger, W.; Breil, L. *Z. Anorg. Allg. Chem.* **1998**, *624*, 1819.
- (10) Bronger, W.; Beissmann, R.; Ridder, G. *J. Alloys Compds.* **1994**, *203*, 91.
- (11) Zhuang, J.; Hastings, J. M.; Corliss, L. M.; Bau, R.; Wei, C. Y.; Moyer, R. O., Jr. *J. Solid State Chem.* **1981**, *40*, 352.
- (12) Moyer, R. O., Jr.; Toby, B. H. *J. Alloys Compds.* **2004**, *363*, 99.
- (13) Bonhomme, F.; Stetson, N. T.; Yvon, K.; Fischer, P.; Hewat, A. *J. Alloys Compds.* **1993**, *200*, 65.
- (14) Černý, R.; Joubert, J.-M.; Kohlmann, H.; Yvon, K. *J. Alloys Compds.* **2002**, *340*, 180.
- (15) Kohlmann, H.; Moyer, R. O., Jr.; Hansen, T.; Yvon, K. *J. Solid State Chem.* **2003**, *174*, 35.
- (16) Davis, J. H.; Jeffrey, K. R.; Bloom, M.; Valic, M. I.; Higgs, T. P. *Chem. Phys. Lett.* **1976**, *42*, 390.
- (17) Abragam, A. *Principles of Nuclear Magnetism*; Clarendon Press: Oxford, 1961; Chapter 10.
- (18) Jacobsen, H.; Berke, H. In *Recent Advances in Hydride Chemistry*; Peruzzini, M., Poli, R., Eds.; Elsevier: The Netherlands, 2001; Chapter 4.
- (19) Bakhmutov, V. I. In *Recent Advances in Hydride Chemistry*; Peruzzini, M., Poli, R., Eds.; Elsevier: The Netherlands, 2001; Chapter 13.
- (20) Nietlispach, D.; Bakhmutov, V. I.; Berke, H. *J. Am. Chem. Soc.* **1993**, *115*, 9191.
- (21) Townes, C. H.; Dailey, B. P. *J. Chem. Phys.* **1949**, *17*, 782.
- (22) Liang, F.; Schmalke, H. W.; Fox, T.; Berke, H. *Organometallics* **2003**, *22*, 3382.
- (23) Firman, T. K.; Landis, C. R. *J. Am. Chem. Soc.* **1998**, *120*, 12650.